VERITAS 2008 - 2009 monitoring of the variable gamma-ray source M 87

V. A. Acciari[1], E. Aliu[2], T. Arlen[3], T. Aune[4], M. Beilicke[5], W. Benbow[1], D. Boltuch[6],
S. M. Bradbury[7], J. H. Buckley[5], V. Bugaev[5], K. Byrum[8], A. Cannon[9], A. Cesarini[10],
Y. C. Chow[3], L. Ciupik[11], P. Cogan[12], W. Cui[13], R. Dickherber[5], C. Duke[14], J. P. Finley[13],
G. Finnegan[15], P. Fortin[2,II], L. Fortson[11], A. Furniss[4], N. Galante[1], D. Gall[13], G. H. Gillanders[10],
S. Godambe[15], J. Grube[9], R. Guenette[12], G. Gyuk[11], D. Hanna[12], J. Holder[6], C. M. Hui[15*],
T. B. Humensky[16], A. Imran[17], P. Kaaret[18], N. Karlsson[11], M. Kertzman[19], D. Kieda[15],
A. Konopelko[20], H. Krawczynski[5], F. Krennrich[17], M. J. Lang[10], S. LeBohec[15], G. Maier[12,℧],
S. McArthur[5], A. McCann[12], M. McCutcheon[12], J. Millis[21,◇], P. Moriarty[22], R. A. Ong[3],
A. N. Otte[4], D. Pandel[18], J. S. Perkins[1], A. Pichel[23], M. Pohl[17,ℵ], J. Quinn[9], K. Ragan[12],
L. C. Reyes[24], P. T. Reynolds[25], E. Roache[1], H. J. Rose[7], A. C. Rovero[23], M. Schroedter[17],
G. H. Sembroski[13], G. Demet Senturk[26], A. W. Smith[8], D. Steele[11,§], S. P. Swordy[16],
M. Theiling[1], S. Thibadeau[5], A. Varlotta[13], S. Vincent[15], R. G. Wagner[8], S. P. Wakely[16],
J. E. Ward[9], T. C. Weekes[1], A. Weinstein[3], T. Weisgarber[16], D. A. Williams[4], S. Wissel[16],
M. Wood[3], B. Zitzer[13]

D. E. Harris[27], F. Massaro[27]

*Corresponding author: C. M. Hui, cmhui@physics.utah.edu

[1]Fred Lawrence Whipple Observatory, Harvard-Smithsonian Center for Astrophysics, Amado, AZ 85645, USA

[2]Department of Physics and Astronomy, Barnard College, Columbia University, NY 10027, USA

[3]Department of Physics and Astronomy, University of California, Los Angeles, CA 90095, USA

[4]Santa Cruz Institute for Particle Physics and Department of Physics, University of California, Santa Cruz, CA 95064, USA

[5]Department of Physics, Washington University, St. Louis, MO 63130, USA

[6]Department of Physics and Astronomy and the Bartol Research Institute, University of Delaware, Newark, DE 19716, USA

[7]School of Physics and Astronomy, University of Leeds, Leeds, LS2 9JT, UK

[8]Argonne National Laboratory, 9700 S. Cass Avenue, Argonne, IL 60439, USA

[9]School of Physics, University College Dublin, Belfield, Dublin 4, Ireland

[10]School of Physics, National University of Ireland Galway, University Road, Galway, Ireland

[11]Astronomy Department, Adler Planetarium and Astronomy Museum, Chicago, IL 60605, USA

[12]Physics Department, McGill University, Montreal, QC H3A 2T8, Canada

[13]Department of Physics, Purdue University, West Lafayette, IN 47907, USA

[14]Department of Physics, Grinnell College, Grinnell, IA 50112-1690, USA

[15]Department of Physics and Astronomy, University of Utah, Salt Lake City, UT 84112, USA

[16]Enrico Fermi Institute, University of Chicago, Chicago, IL 60637, USA

[17]Department of Physics and Astronomy, Iowa State University, Ames, IA 50011, USA

[18]Department of Physics and Astronomy, University of Iowa, Van Allen Hall, Iowa City, IA 52242, USA

[19]Department of Physics and Astronomy, DePauw University, Greencastle, IN 46135-0037, USA

[20]Department of Physics, Pittsburg State University, 1701 South Broadway, Pittsburg, KS 66762, USA

[21]Department of Physics, Anderson University, 1100 East 5th Street, Anderson, IN 46012

[22]Department of Life and Physical Sciences, Galway-Mayo Institute of Technology, Dublin Road, Galway, Ireland

[23]Instituto de Astronomia y Fisica del Espacio, Casilla de Correo 67 - Sucursal 28, (C1428ZAA) Ciudad Autnoma de Buenos Aires, Argentina

[24]Kavli Institute for Cosmological Physics, University of Chicago, Chicago, IL 60637, USA

[25]Department of Applied Physics and Instrumentation, Cork Institute of Technology, Bishopstown, Cork, Ireland

[26]Columbia Astrophysics Laboratory, Columbia University, New York, NY 10027, USA

[27]Smithsonian Astrophysical Observatory, 60 Garden St., Cambridge, MA 02138, USA

[II]Now at Laboratoire Leprince-Ringuet, Ecole Polytechnique, CNRS/IN2P3, F-91128 Palaiseau, France

[ʊ]Now at DESY, Platanenallee 6, 15738 Zeuthen, Germany

[◇]Now at Department of Physics, Anderson University, 1100 East 5th Street, Anderson, IN 46012

ABSTRACT

M 87 is a nearby radio galaxy that is detected at energies ranging from radio to very-high-energy (VHE) gamma-rays. Its proximity and its jet, misaligned from our line-of-sight, enable detailed morphological studies and extensive modeling at radio, optical, and X-ray energies. Flaring activity was observed at all energies, and multi-wavelength correlations would help clarify the origin of the VHE emission. In this paper, we describe a detailed temporal and spectral analysis of the VERITAS VHE gamma-ray observations of M87 in 2008 and 2009. In the 2008 observing season, VERITAS detected an excess with a statistical significance of 7.2 standard deviations (σ) from M 87 during a joint multi-wavelength monitoring campaign conducted by three major VHE experiments along with the Chandra X-ray Observatory. In February 2008, VERITAS observed a VHE flare from M 87 occurring over a 4-day timespan. The peak nightly flux above $250\,\mathrm{GeV}$ was $(1.14 \pm 0.26) \times 10^{-11}\mathrm{cm}^{-2}\mathrm{s}^{-1}$, which corresponded to 7.7% of the Crab Nebula flux. M 87 was marginally detected before this 4-day flare period, and was not detected afterwards. Spectral analysis of the VERITAS observations showed no significant change in the photon index between the flare and pre-flare states. Shortly after the VHE flare seen by VERITAS, the Chandra X-ray Observatory detected the flux from the core of M 87 at a historical maximum, while the flux from the nearby knot HST-1 remained quiescent. Acciari et al. (2009) presented the 2008 contemporaneous VHE gamma-ray, Chandra X-ray, and VLBA radio observations which suggest the core as the most likely source of VHE emission, in contrast to the 2005 VHE flare that was simultaneous with an X-ray flare in the HST-1 knot. In 2009, VERITAS continued its monitoring of M 87 and marginally detected a $4.2\,\sigma$ excess corresponding to a flux of $\sim 1\%$ of the Crab Nebula. No VHE flaring activity was observed in 2009.

Subject headings: gamma rays: galaxies — galaxies: individual (M 87, VER J1230+123)

1. Introduction

M 87 is an FR I radio galaxy located at a distance of $16.7\,\mathrm{Mpc}$, near the center of the Virgo cluster. It has been observed at all wavelengths ranging from radio to VHE gamma rays. Its core is an active galactic nucleus (AGN) powered by a supermassive black hole of mass $(6.0\pm0.5)\times10^9\,\mathrm{M}_\odot$ (Gebhardt & Thomas 2009) (see supporting material of Acciari et al. (2009) for mass corrected for our distance assumption), which is the source from which the first plasma jet emission was observed

---

[א]Now at Institut für Physik und Astronomie, Universität Potsdam, 14476 Potsdam-Golm,Germany; DESY, Platanenallee 6, 15738 Zeuthen, Germany

[§]Now at Los Alamos National Laboratory, MS H803, Los Alamos, NM 87545

(Curtis 1918). Most of the known extragalactic VHE sources are blazars (TeVCat 2007), AGN with a jet aligned close to the line-of-sight; on the contrary, the jet of M 87 is misaligned. Apparent superluminal motion was observed in both the radio (Cheung et al. 2007) and optical (Biretta et al. 1999) bands for different features along the jet, constraining the jet orientation to less than $30°$ from the line-of-sight at the location of the HST-1 knot, which is located 0.86" from the core (Harris et al. 2009).

VHE emission from M 87 was first reported by the HEGRA collaboration at a statistical significance of $4.1\,\sigma$ during their $1998-1999$ observations (Aharonian et al. 2003). This was confirmed by the H.E.S.S. collaboration (Aharonian et al. 2006), which additionally reported year-scale flux variability. The observed variability provides a size constraint on the VHE emission production region and disfavors large-scale gamma-ray production models, such as the dark matter annihilation model (Baltz et al. 2000) and the interacting cosmic-ray proton scenario (Pfrommer & Ensslin 2003) which predict steady gamma-ray emission. However, the angular resolution of imaging atmospheric Cherenkov telescopes (IACTs) is insufficient to resolve any structure in M 87. Aharonian et al. (2006) also reported fast (2-day scale) variability during a high state of gamma-ray activity in 2005, which further constrains the VHE emission size and favors the immediate vicinity of the M 87 black hole as the VHE production site; on the other hand, Chandra X-ray observations at the time of the VHE flare indicated a different scenario. Strong flux variability from both the core and HST-1 in the energy range $0.2-6\,\mathrm{keV}$ has been detected by Chandra M 87 monitoring since 2002 (Harris et al. 2003). At the same period of the flare observed by H.E.S.S. in 2005, Harris et al. (2008) reported an X-ray flux from HST-1 at more than 50 times the intensity observed in 2000, along with flaring activity observed in ultraviolet and radio wavelengths, suggesting the HST-1 knot as a more likely source of VHE emission than the core.

The All-Sky Monitor (ASM) on the Rossi X-ray Timing Explorer (RXTE) has provided daily monitoring of M 87 in the energy range $2-12\,\mathrm{keV}$ since 1996. However, ASM cannot resolve the core and the HST-1 knot. A year-scale correlation between the annual ASM/RXTE X-ray flux and the VHE gamma-ray flux recorded over the past 10 years was reported by Acciari et al. (2008). The core was presented as the more favorable VHE production site over HST-1 based on this year-scale correlation, and the non-detection of the 2005 flare in the HST-1 knot by ASM. However, no year-scale correlation has been seen with Chandra data of the M 87 core or the HST-1 knot over the past 5 years in the $0.2-6\,\mathrm{keV}$ range. The ASM/RXTE quick-look results do not show any correlated activity with VHE observations at shorter time scales, as a result of the limited sensitivity of ASM.

The proximity of M 87 and its misaligned jet enable high resolution studies of its jet structures in radio, optical, and X-rays (Marshall et al. 2002) (Perlman & Wilson 2005). The jet morphology is similar in those wavebands, and leptonic synchrotron radiation is favored as the process for non-thermal emission within the jet (Wilson & Yang 2002). Based on the multiwavelength correlated activities and variability studies, the favored candidate for VHE emission is the small-scale (sub-arcsecond) jet region. Reimer et al. (2004) propose a synchrotron-proton blazar model in which protons are accelerated to energies above EeV and emit gamma rays via muon/pion synchrotron

or proton synchrotron radiation. However, this model requires a strong magnetic field to accelerate the protons to such high energies, and the predicted VHE spectrum is steeper than observed. Several leptonic models involving synchrotron and inverse Compton (IC) radiation have also been suggested, with the multi-component emission originating in the inner jet: there is the model by Georganopoulos et al. (2005) in which energetic electrons IC scatter off of synchrotron photons produced downstream in the decelerating jet; a scenario by Lenain et al. (2008) in which VHE emission is produced via the synchrotron self-Compton (SSC) process inside several similar homogenous compact components which contain more energetic electrons than the jet; and the model by Tavecchio & Ghisellini (2008), in which a fast-moving spine is surrounded by a slower-moving sheath, producing VHE emission via external-Compton scattering. Single-component SSC emission is recently modelled by Abdo et al. (2009) with VLBA radio, Chandra X-ray, and Fermi LAT 2009 data. However, comparing the model to archival non-flaring VHE data, it appears to underpredict the VHE emission.

The vicinity of the black hole (the core) has been suggested by Levinson (2000) and Neronov & Aharonian (2007) in the black hole magnetosphere model, in which gamma-ray photons are produced by electrons accelerated by the electromagnetic field of the black hole. The HST-1 knot, 0.86" away from the core, has also been demonstrated as a possible location for jet reconfinement where photons can be upscattered to TeV energies via IC process (Stawarz et al. 2006).

In 2008, the VHE gamma-ray experiments H.E.S.S., MAGIC, and VERITAS took part in a joint multi-wavelength monitoring campaign of M 87 along with Chandra (Beilicke et al. 2008). The VHE observations were closely coordinated in order to guarantee a reasonable coverage around the Chandra pointings and a well sampled VHE light curve during the first half of 2008. During this joint monitoring campaign, MAGIC reported flaring activities during a 13-day observation period between January 30 (MJD 54495) and February 11 (MJD 54507), with day-scale variability occurring throughout the duration of the flare (Albert et al. 2008). Subsequently, the VERITAS collaboration triggered intensified observations of M 87, and detected a 4-day flare from February 9 (MJD 54505) to February 13 (MJD 54509). The VHE and Chandra X-ray light curves of the joint campaign, along with a coincident VLBA radio light curve, are presented in Acciari et al. (2009), which also include a discussion on the radio/VHE gamma-ray correlation as evidence that the VHE emission originates from the core.

The VHE flux monitoring campaign continued in 2009 with MAGIC and VERITAS. In this paper, we present the results from two seasons (2008 − 2009) of VERITAS observations, along with a full analysis on the time scale of the flux variability, and a search for spectral variability in the 2008 data set when the VHE flaring activity was observed.

2. Observations and Analysis

VERITAS, the Very Energetic Radiation Imaging Telescope Array System, is an array of four 12 m diameter IACTs located at the Fred Lawrence Whipple Observatory on Mount Hopkins ($31°40'$ N, $110°57'$ W) at an altitude of 1.3 km above sea level. Each telescope has a total area of $110\,\mathrm{m}^2$ and an f/D ratio of 1.0. Each telescope camera is equipped with 499 photomultiplier tubes, arranged in a hexagonal lattice covering a field of view (FOV) of $3.5°$. The array is sensitive from $\sim100\,\mathrm{GeV}$ to more than 30 TeV, with an effective area of up to $10^5\,\mathrm{m}^2$ and an angular resolution of $0.1°$ at 1 TeV (68% containment). VERITAS can detect a source with 1% Crab Nebula flux in less than 50 hours, and a source with 5% Crab Nebula flux in ~2.5 hours. For more technical details of VERITAS, see Holder et al. (2006).

M 87 was observed with VERITAS for over 43 hours between December 2007 and May 2008 and over 25 hours between January and May 2009, at a range of zenith angles from $19°$ to $41°$. All of 2008 data and 81% of 2009 data used were taken with 4 telescopes, while 19% of 2009 data were taken with only a 3-telescope array. After eliminating observations in poor weather and those with an unstable trigger rate, 37 hours and 19 hours of good quality live time remain in 2008 and 2009, respectively.

Shower images from all working telescopes are first corrected in gain and timing using parameters obtained from the nightly laser calibration data (Hanna et al. 2007). The images are then passed through a two-step cleaning process that retains pixels with a signal that is several times higher than the night-sky background level. Each shower image is then parametrized (Hillas 1985), and the shower direction is reconstructed using the stereoscopic technique (Hofmann et al. 1999). Events are then selected as gamma-ray-like if at least three camera images pass the standard cuts optimized for a 10% Crab Nebula flux source (Colin et al. 2008). All the observations were performed in "wobble mode" where M 87 was tracked with a $0.5°$ offset relative to the camera such that the camera's FOV contain both the source region and regions for background estimation. The on-source region is defined by a $0.15°$ radius circle centered on the M 87 core. All gamma-ray-like events within this region are summed (ON count) and the background estimated from seven identically sized regions reflected from the source region around the camera center is also summed (OFF count) (Berge et al. 2007). The ON and OFF counts are then used in Formula 17 of Li & Ma (1983) to calculate the significance of the excess. As a standard procedure in VERITAS, the results were confirmed by at least one independent analysis package (Daniel et al. 2007) which was presented in Acciari et al. (2009).

3. Results

3.1. 2008

The VERITAS observations in 2008 resulted in 450 excess events, corresponding to a statistical significance of $7.2\,\sigma$. The average flux above $250\,\mathrm{GeV}$ is $(2.74\pm0.61)\times10^{-12}\,\mathrm{cm}^{-2}\,\mathrm{s}^{-1}$, corresponding to 1.8% of the Crab Nebula flux. The differential energy spectrum of M 87 measured by VERITAS in 2008 is consistent with a power-law distribution $dN/dE = \Phi_0(E/\mathrm{TeV})^{-\Gamma}$, with $\Phi_0 = (5.17 \pm 0.91_{stat} \pm 1.03_{syst}) \times 10^{-13}\,\mathrm{cm}^{-2}\,\mathrm{s}^{-1}\,\mathrm{TeV}^{-1}$ and $\Gamma = 2.49 \pm 0.19_{stat} \pm 0.20_{syst}$. The χ^2/dof for the power-law fit is 3.1/4.0. The measured photon index is consistent with reported measurements from Aharonian et al. (2006), Acciari et al. (2008), and Albert et al. (2008) ranging from 2.22 to 2.62 with statistical uncertainties between 0.11 and 0.35. Table 1 lists the differential flux points measured by VERITAS in 2008.

The 2008 VERITAS light curve is shown in Fig. 1 assuming the average fitted photon index of 2.50. The χ^2/dof of a constant rate fit to the entire dataset is 52/26, rejecting the constant flux hypothesis at 99.9% confidence level. On Feb 9 (MJD 54505), M 87 was detected at over $4\,\sigma$ after 2 hours of observation and a trigger alert was sent out to other collaborations for intensified observations. The peak flux of the VERITAS dataset occured on the night of Feb 12 (MJD 54508) at $(1.14 \pm 0.26) \times 10^{-11}\mathrm{cm}^{-2}\mathrm{s}^{-1}$ above $250\,\mathrm{GeV}$, equivalent to 7.7% of the Crab Nebula flux. The flare period is defined by the nights removed from the whole dataset such that the constant rate fit to the rest of the lightcurve reaches a χ^2/dof close to 1. The nights that meet the criteria for the flare period are Feb 9, 10, 12, and 13 (MJD $54505 - 54509$). The dataset is then further split into pre-flare and post-flare period.

During the flare period, M 87 was observed for 5.4 hours of live time and was detected at $7.4\,\sigma$ (pre-trials). The flux above $250\,\mathrm{GeV}$ during the flare period was $(7.59 \pm 1.11) \times 10^{-12}\,\mathrm{cm}^{-2}\,\mathrm{s}^{-1}$, corresponding to 5.1% of the Crab Nebula flux. The 99% confidence interval for the flux during

Table 1.   M 87 differential flux measured between December 2007 and May 2008 by VERITAS.

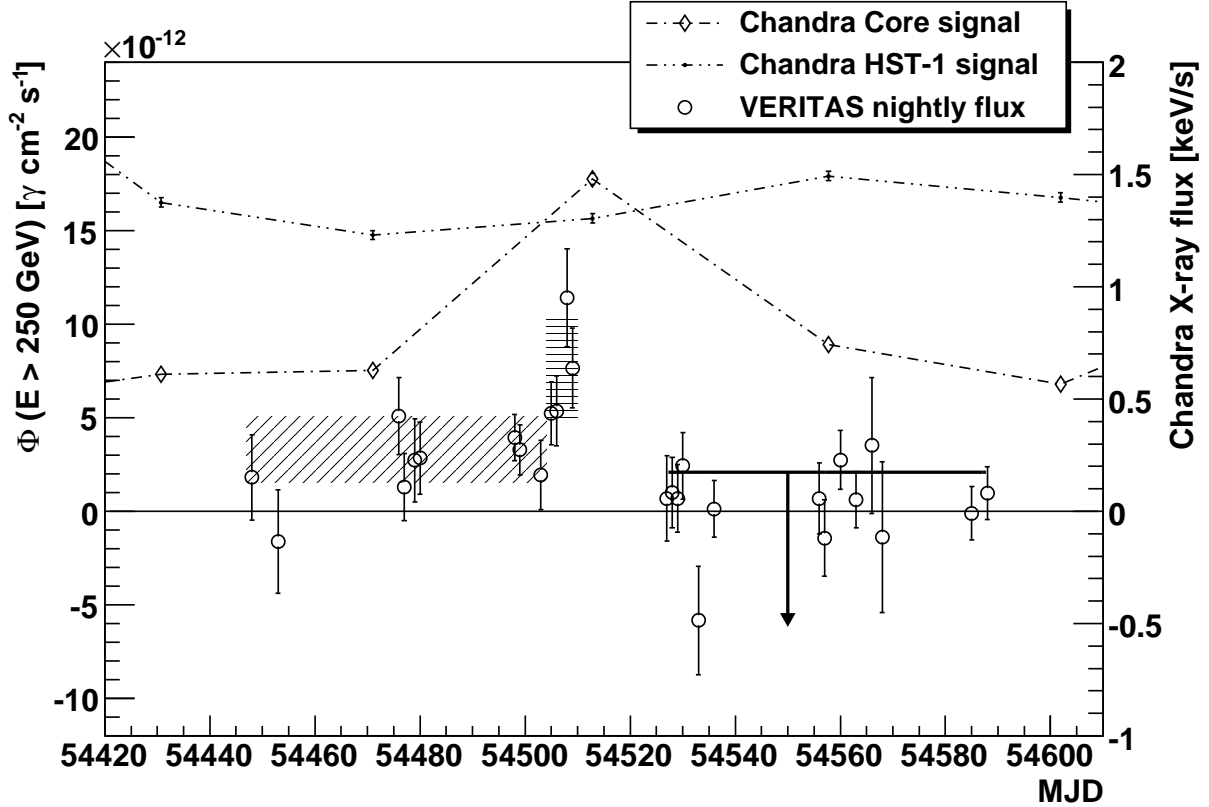| Energy [TeV]	Differential Flux [$\mathrm{cm}^{-2}\,\mathrm{s}^{-1}\,\mathrm{TeV}^{-1}$]	Significance [σ]
0.24	$(1.99 \pm 0.54) \times 10^{-11}$	3.68
0.42	$(3.56 \pm 1.16) \times 10^{-12}$	3.07
0.75	$(1.51 \pm 0.34) \times 10^{-12}$	4.44
1.33	$(1.70 \pm 0.95) \times 10^{-13}$	1.79
2.37	$(6.02 \pm 3.40) \times 10^{-14}$	1.78
4.22	$(1.72 \pm 1.13) \times 10^{-14}$	1.52

Fig. 1.— VERITAS night-by-night VHE gamma-ray flux and Chandra X-ray flux (Harris et al. 2009) from the core and from the HST-1 knot of M 87 in 2008. The flare period (MJD 54505−54509, Feb 9 − 13) seen in VHE gamma rays coincides with a historically high state of the core in X-rays, while the HST-1 knot remains in a low flux state. The black slant-lined area shows the 99% confidence intervals of the pre-flare period; the black horizontal-lined area shows the 99% confidence intervals of the flare period; the black line with the arrow indicates the upper limit of the post-flare period at 99% confidence level (Helene 1983).

the flare period (see horizontal-lined area between MJD 54505 and 54509 in Fig. 1) is between $4.73 \times 10^{-12}\,\mathrm{cm^{-2}\,s^{-1}}$ and $10.45 \times 10^{-12}\,\mathrm{cm^{-2}\,s^{-1}}$.

Before the flare period (MJD $54448 - 54503$), which included two nights immediately after the major flare observed by MAGIC (Albert et al. 2008), M 87 was marginally detected with 13.8 hours of live time at a flux of $(3.30 \pm 0.68) \times 10^{-12}\,\mathrm{cm^{-2}\,s^{-1}}$ above 250 GeV. The 99% confidence interval for the flux during the pre-flare period (see slant-lined area between MJD 54448 and 54503 in Fig. 1) is between $1.55 \times 10^{-12}\,\mathrm{cm^{-2}\,s^{-1}}$ and $5.05 \times 10^{-12}\,\mathrm{cm^{-2}\,s^{-1}}$. M 87 was observed for an additional 17.2 hours of live time after the flare period and was not detected. An upper limit of $2.1 \times 10^{-12}\,\mathrm{cm^{-2}\,s^{-1}}$ at 99% confidence level (Helene 1983) is established for the post-flare period, corresponding to 1.4% of the Crab Nebula flux. Assuming a normal distribution for the flux measurement, the flare flux is higher than the pre-flare flux at 99.95% confidence level, and the pre-flare flux is higher than the post-flare flux at 99.8% confidence level. All of the above calculations were performed under the assumption of a constant photon index of 2.50.

The spectra from different periods are plotted in Fig. 2 and there is no indication of a spectral cut-off. The power-law fit parameters from the overall, flare, and pre-flare spectra are displayed in Table 2. No significant difference in photon index and photon energy distribution is found between the flare and pre-flare states.

To test if there is any correlation between the spectral flux and photon index measured during different activity levels corresponding to the core, a linear test function of the form $\Gamma = p_0 + p_1 \times \log 10\,\Phi_0$ was fitted to past measurements by Aharonian et al. (2006) in 2004 and Acciari et al. (2008) in 2007, and the high/low states measured by Albert et al. (2008) and by VERITAS in 2008 (see Fig. 3). The measurement by HESS in 2005 is excluded in the fit due to possible contamination from the HST-1 flare. The χ^2/dof of the linear fit is 1.7/4 and the corresponding probability of a correlation between photon index and flux is 78.6%. The fit parameter p_1 is consistent with zero. Fitting a constant photon index gave a χ^2/dof of 2.7/5 and a corresponding probability of 74.6%. No significant correlation is found between the photon index and the flux.

At the time of the flare detected by VERITAS, Chandra measured the core X-ray flux at a historical maximum, at $4.1\,\sigma$ above the mean core flux between 2000 and 2009, and exceeding the

Table 2. Power-law fit parameters of the VHE spectrum of M 87 in different epochs during 2008.

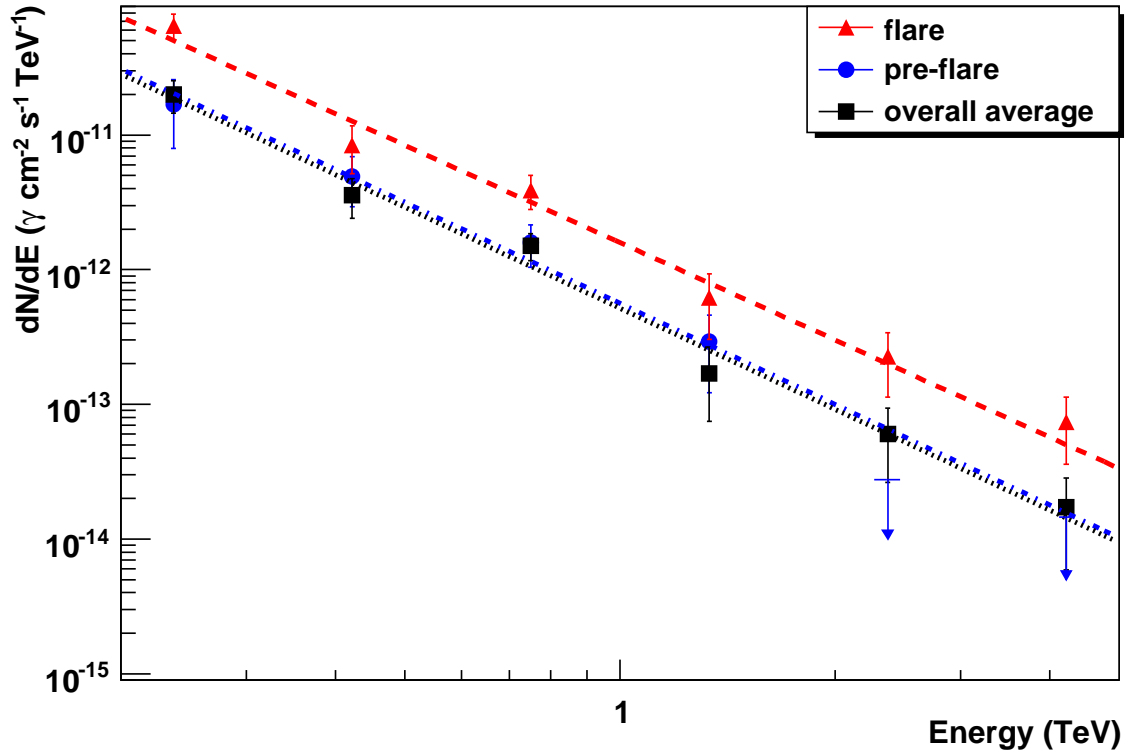| Data Set	Φ_0 $[10^{-13}\,\mathrm{cm^{-2}\,s^{-1}\,TeV^{-1}}]$	Γ	χ^2/dof
2008 overall	5.2 ± 0.9	2.5 ± 0.2	3.1/4
flare state	15.9 ± 2.9	2.4 ± 0.2	3.9/4
pre-flare state	5.6 ± 1.5	2.5 ± 0.3	1.3/4

Fig. 2.— Spectra of M87 measured at different periods by VERITAS. Data points less than $1.5\,\sigma$ are represented as upper limits. The power-law fit parameters are listed in Table 2. The photon energy distribution is consistent throughout different activity levels, and there is no indication of a spectral cut-off.
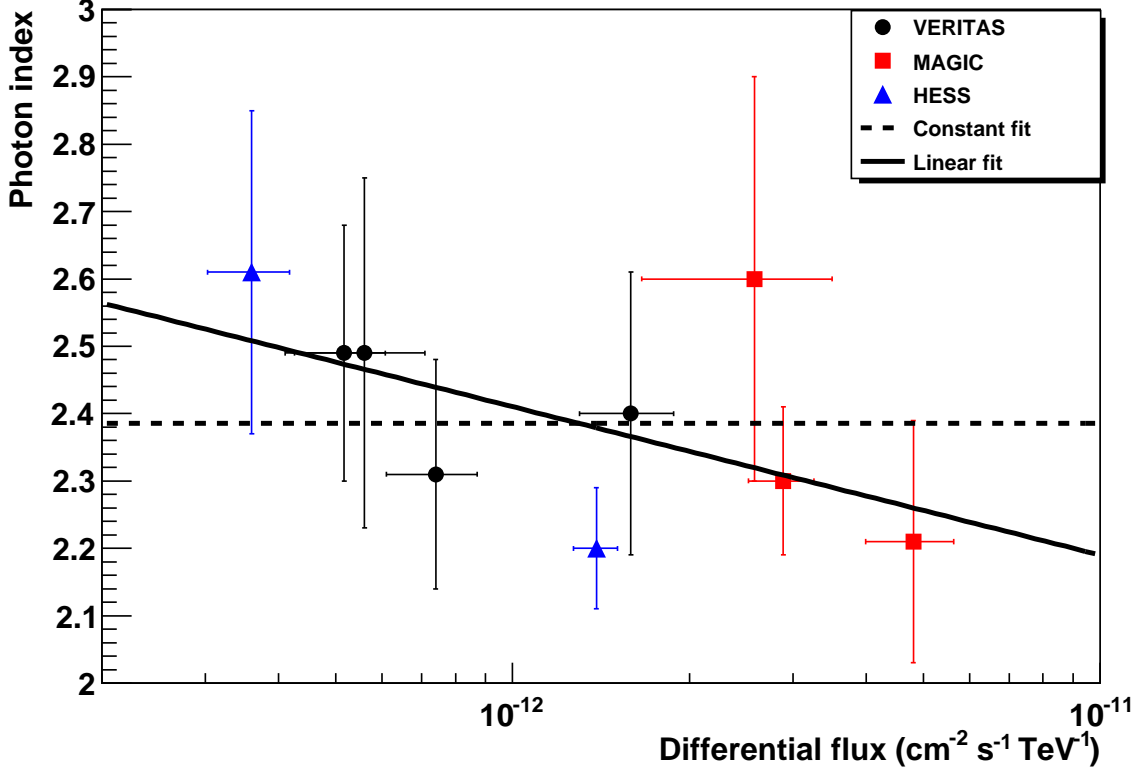
Fig. 3.— Photon index versus differential flux as reported by HESS in 2004 and 2005 (Aharonian et al. 2006), by MAGIC in 2008 (overall, flare, and non-flare) (Albert et al. 2008), and by VERITAS in 2007 (Acciari et al. 2008) and 2008 (overall, flare, and pre-flare). All spectra are compatible within their statistical errors. A linear coorelation fit between photon index and flux has the same probability as a constant photon index fit.

flux from the HST-1 knot (see Fig. 1 and 4) (Harris et al. 2009). The peak core X-ray flux measured by Chandra during the observation period of VERITAS was 2.3 times the average core X-ray flux, with the average calculated excluding this flare data point. While the HST-1 knot X-ray flux during this period fluctuated $\pm 10\%$ from the average and is relatively steady when compared to the core emission. Fig. 5 shows the fractional change per year (fpy) first presented in Harris et al. (2009). Around the 2008 VHE gamma-ray flare period, the Chandra core fpy is more variable than that of the Chandra HST-1 fpy measurement. The definition of fpy is repeated below (Harris et al. 2009).

$$\mathrm{fpy} = \frac{I_2 - I_1}{I_i \Delta t} \qquad (1)$$

$$\sigma_{\mathrm{fpy}} = \frac{1}{\Delta t} \times \frac{I_j}{I_i} \times \sqrt{(\frac{\sigma_1}{I_1})^2 + (\frac{\sigma_2}{I_2})^2} \qquad (2)$$
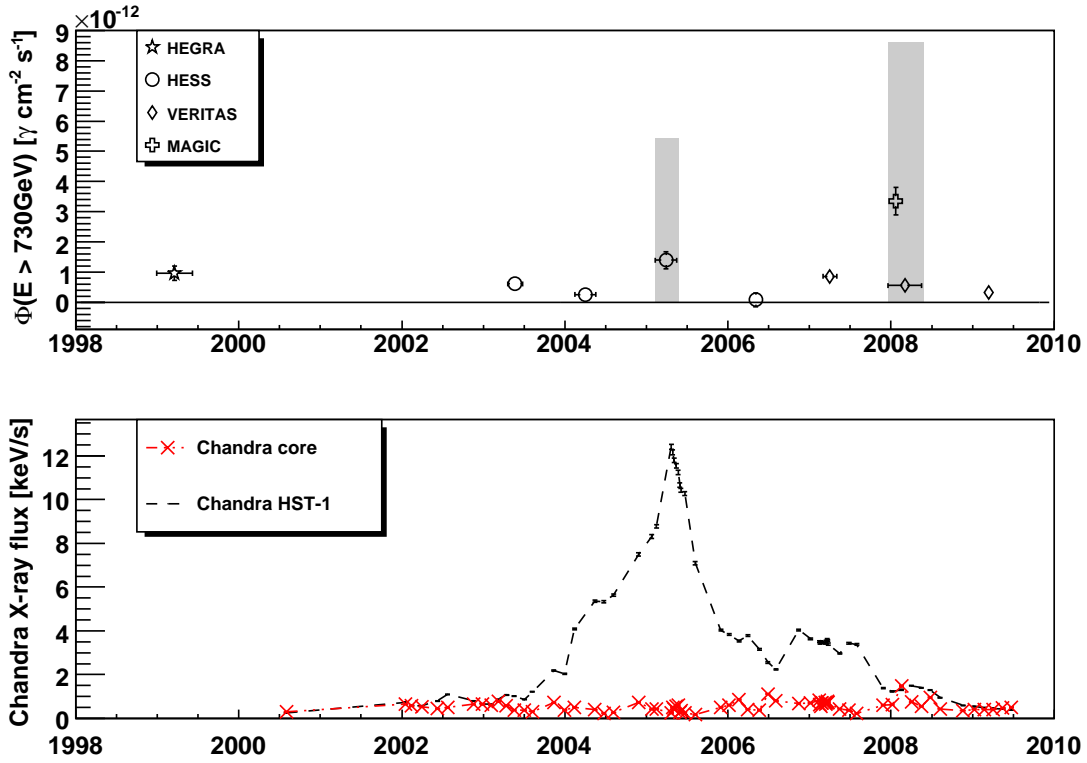
Fig. 4.— M 87 yearly VHE gamma-ray (Aharonian et al. 2003) (Aharonian et al. 2006) (Acciari et al. 2008) (Albert et al. 2008) and X-ray fluxes (Harris et al. 2009). The VHE gamma-ray flux is for energy >730 GeV due to the original flux scale used in the HEGRA paper. This yearly flux plot is first presented in (Acciari et al. 2008) and is now updated with 2008 and 2009 data. Grey areas represent the range of variable VHE fluxes observed that year to give a more accurate picture of the flux level of M87.

where I is the X-ray intensity measured by Chandra and Δt is the time between the two intensity measurements in units of year. If the X-ray intensity is increasing (i.e. $I_2 > I_1$), then $i = 1, j = 2$; if the X-ray intensity is decreasing ($I_2 < I_1$), then $i = 2, j = 1$.

3.2. 2009

The VERITAS observations in 2009 resulted in 134 excess events at a significance of $4.2\,\sigma$. The χ^2/dof of a constant rate fit to the entire dataset is $23/18$ and no significant variability was observed in the 2009 data set. The average flux above $250\,\mathrm{GeV}$ is $(1.59 \pm 0.39) \times 10^{-12}\,\mathrm{cm}^{-2}\,\mathrm{s}^{-1}$ assuming a photon index of 2.50. This corresponds to 1.1% of the Crab Nebula flux and is consistent with the reported Fermi-LAT spectrum (Abdo et al. 2009). The 2009 flux is below the 2008 pre-flare flux at the 98.5% confidence level, but above the 2008 post-flare flux at the 87.6% confidence level. Fig. 5 shows the light curves of both 2008 and 2009 observed by VERITAS and the X-ray flux measured by Chandra for the core and the knot HST-1, along with the fpy of Chandra X-ray flux.

During the 2009 observation period, Chandra took a flux measurement every $40-50$ days. The HST-1 flux measured by Chandra is steadily declining at a rate of $5-10\%$ when compared to the previous flux ($\delta I/I_1$). The core flux, however, is mostly increasing by as much as 18%. The lack of VHE activity during this period suggests a possible association between VHE flares and significant changes in the X-ray flux such as the one seen in 2008 where the core fpy is more variable than in 2009 (see Fig. 5).

4. Discussion

The proximity of M 87 and its misaligned jet have enabled the study of its jet morphology in a broad range of energies. Flaring activities from individual jet features have been observed in radio, optical, and X-rays in parallel (Cheung et al. 2007). Modeling of the particle acceleration yields several possible VHE emission origins. Even though the VHE gamma-ray technique cannot resolve individual features of M 87, the rapid variability reported by Aharonian et al. (2006) and Albert et al. (2008) has constrained the size of the VHE emission region to $< 2.6\,\delta\,\mathrm{R_s}$ where δ is the relativistic Doppler factor and R_s the Schwarzschild radius of the M 87 black hole ($\mathrm{R}_s \sim 10^{15}\mathrm{cm}$). During the 2008 joint monitoring campaign of M87, VERITAS observed a gamma-ray flare in February 2008 which spanned 4 days, constraining the emission region size to $\mathrm{R} \leq \mathrm{R_{var}} = \delta\,\mathrm{c}\,\Delta\mathrm{t}/(1 + \mathrm{z}) \approx \delta\,10^{16}\mathrm{cm}$. Radio observations have shown evidence that charged particles are accelerated in the immediate vicinity of the black hole closer than $100\,R_s$ (Acciari et al. 2009). Combining these radio observations with the size constraint from the VERITAS 2008 data, we can constrain the relativistic Doppler factor $\delta \leq 10$ with the flaring activity measured by VERITAS.

The VHE emission size constraint narrows down the most probable VHE emission location to either the unresolved core region or the HST-1 knot. X-ray time scale analysis presented by
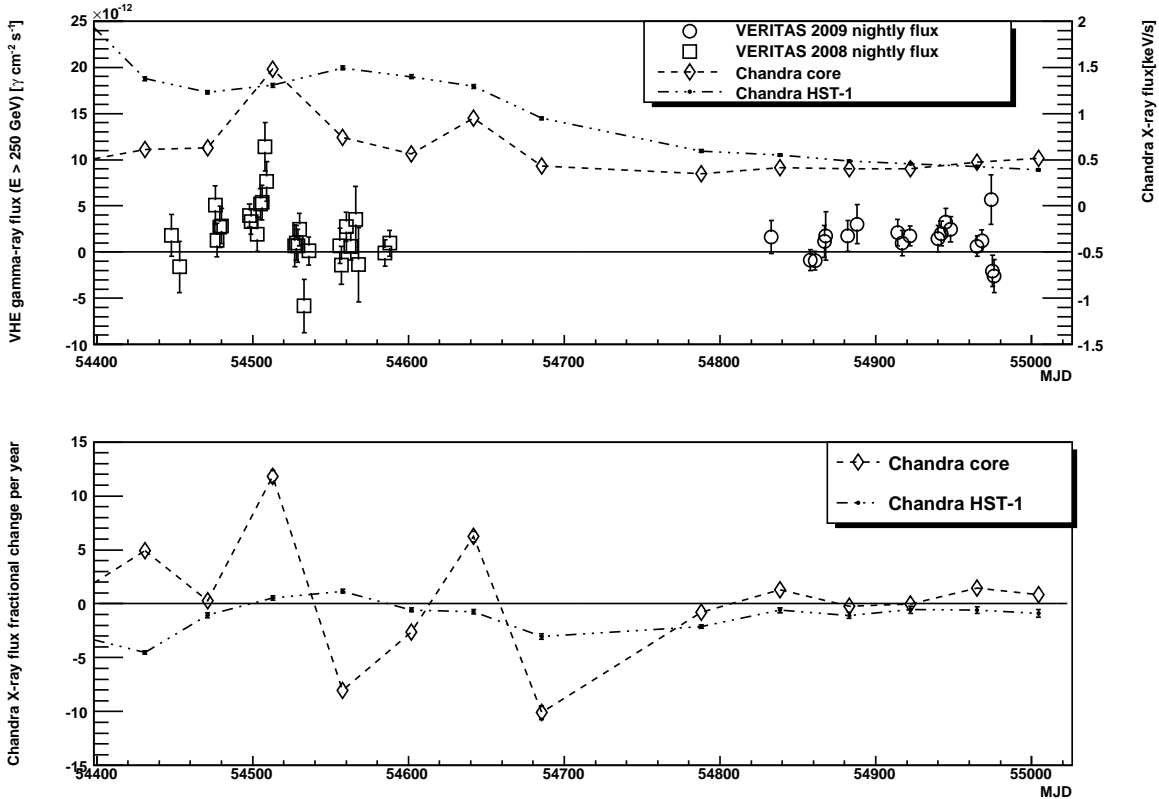
Fig. 5.— *Upper panel:* VERITAS night-by-night VHE gamma-ray flux and Chandra X-ray flux from the core and from the HST-1 knot of M 87 in 2008 (Harris et al. 2009) and 2009. *Lower panel:* Chandra X-ray flux fractional change per year, see text for definition (Harris et al. 2009).

Harris et al. (2009) suggests the X-ray emission size of the core to be smaller than that of HST-1. However the upper limits on the X-ray emission region size from the time scale analysis are still larger than the VHE emission size inferred from the VHE variability time scales reported previously. Therefore, both HST-1 and the core region remain as the possible origins of VHE emission.

In 2009 VERITAS detected M87 similar to the 2008 pre-flare level. The X-ray time scale analysis is repeated for the 2009 Chandra data and the fractional change per year (fpy) for the core in 2009 is smaller than in 2008 during the VHE gamma-ray flare. The fpy of the knot HST-1 appeared to be negative throughout 2008 and 2009, and at a smaller amplitude than the core. This may be an indication of correlation between large X-ray flux changes and flaring activities in VHE gamma rays. It should be noted however, that large fpy in the core was observed by Chandra as well in 2007 with no corresponding VHE gamma-ray flare. A similar analysis is not performed for the 2005 HESS flare due to contamination from the knot HST-1 in Chandra data.

The compactness of the particle accelerators operating in the vicinity of the supermassive

black hole and the absence of a significant cut-off in the spectrum imply that the particle acceleration mechanism is highly efficient. Levinson (2000), Neronov & Aharonian (2007), and others have argued that acceleration mechanisms similar to those in pulsar magnetosphere models can also operate in the black hole magnetosphere. The black hole magnetosphere model and the two-zone leptonic models (Georganopoulos et al. 2005) (Lenain et al. 2008) (Tavecchio & Ghisellini 2008) can reproduce the VHE spectrum and the flux variability well. While no constraints can be placed on the VHE range of these models, since VERITAS and other VHE gamma-ray instruments did not observe a cut-off in the spectrum of M 87, the Fermi gamma-ray telescope, sensitive from MeV to GeV energies, can potentially provide constraints on the magnetic field strength and a measure of low-energy gamma-ray photon flux from the synchrotron/curvature radiation. Abdo et al. (2009) presented the first year of Fermi-LAT observations of M87 in 2009 during its quiescent state. Continual monitoring in all wavelength is essential for the modelling of the spectral energy distribution of M87. Future instruments such as CTA/AGIS, with their improved sensitivity, can potentially detect shorter time scale variability and further constrain the size of the VHE emission region.

Begelman (2009) provided a concise commentary on the M 87 2008 multi-wavelength results and the importance of multi-wavelength observations to understanding particle acceleration mechanisms near black holes. The high-resolution imaging of radio telescopes, combined with VHE gamma-ray observations from ground-based instruments, have shown the first association between a VHE gamma-ray flare and an increase in radio flux coming from a region very close to the black hole (Acciari et al. 2009). This coincident multi-wavelength coverage led to several modeling discussions of the joint VHE and radio light curves (see supplement of Acciari et al. (2009)). Even with M 87 day-scale VHE flux variability and additional constraints from radio and X-ray observations, there remains several plausible models, which explain how particles are accelerated to very high energies near the black hole and how the consequent radiation is able to reach us. Multi-wavelength monitoring work is being continued, and is essential to address these questions.

Facilities: CXO, HEGRA, HESS, MAGIC, VERITAS

REFERENCES

Abdo, A. A., et al. 2009, ApJ, 707, 55

Acciari, V. A., et al. 2009, Science, 325, 444

Acciari, V. A., et al. 2008, ApJ, 679, 397

Aharonian, F., et al. 2003, A&A, 403, L1

Aharonian, F., et al. 2006, Science, 314, 1424

Albert, J., et al. 2008, ApJ, 685, L23

Baltz, E. A., Briot, C., Salati, P., Taillet, R., & Silk, J. 2000, Phys. Rev. D, 61, 023514

Begelman, M. 2009, Science, 325, 399

Beilicke, M., et al. 2008, in AIP Conf. Proc. 1085, 4th International Meeting on High Energy
    Gamma-ray Astronomy, 553

Berge, D., Funk, S., & Hinton, J. 2007, A&A, 466, 1219

Biretta, J. A., Sparks, W. B., & Macchetto, F. 1999, ApJ, 520, 621

Cheung, C. C., Harris, D. E., Stawarz, L. 2007, ApJ, 663, L65

Colin, P., et al. 2008, in 30th ICRC Proc., 3, 997

Curtis, H. D. 1918, Publ. Lick Obs., 13, 9

Daniel, M. K., et al. 2007, in 30th ICRC Proc., 3, 1325

Georganopoulos, M., Perlman, E. S., & Kazanas, D. 2005, ApJ, 634, L33

Gebhardt, K., & Thomas, J. 2009, ApJ, 700, 1690

Hanna, D., et al. 2007, in 30th ICRC Proc., 3, 1417

Harris, D. E., Cheung, C. C., Stawartz, L., Biretta, J. A., & Perlman, E. S. 2009, ApJ, 699, 305

Harris, D. E., Cheung, C. C., Stawarz, L., Biretta, J. A., Sparks, W., Perlman, E. S., & Wilson,
    A. S. 2008, in ASP Conf. Ser. 386, Extragalactic Jets, 80

Harris, D. E., Biretta, J. A., Junor, W., Perlman, E. S., Sparks, W. B., & Wilson, A. S. 2003, ApJ,
    586, L41

Helene, O. 1983, Nuclear Instruments & Methods, 212, 319

Hillas, A. M. 1985, in 19th ICRC Proc., 3, 445

Hofmann, W., et al. 1999, Astropart. Phys., 12, 135

Holder, J., et al. 2006, Astropart. Phys., 25, 391

Lenain, J.-P., Boisson, C., Sol, H., & Katarzynski, K. 2008, A&A, 478, 111

Levinson, A. 2000, Phys. Rev. Lett., 85, 5

Li, T. P., & Ma, Y. Q. 1983, ApJ, 272, 317

Marshall, H. L., et al. 2002, ApJ, 564, 683

Neronov, A., & Aharonian, F. A. 2007, ApJ, 671, 85

Perlman, E. S., & Wilson, A. S. 2005, ApJ, 627, 140

Pfrommer, C., & Ensslin, T. A. 2003, A&A, 407, L73

Reimer, A., Protheroe, R. J., & Donea, A.-C., 2004, A&A, 419, 89

Stawarz, L., Aharonian, F., Kataoka, J., Ostrowski, M., Siemiginowska, A., & Sikora, M. 2006, MNRAS, 370, 981

Tavecchio, F., & Ghisellini, G. 2008, MNRAS, 385, L98

TeVCat, Online Gamma-Ray Catalog, http://tevcat.uchicago.edu

Wilson A. S., & Yang Y. 2002, ApJ, 568, 133